



1 **Impact of bioenergy crops expansion on climate-carbon cycle** 2 **feedbacks in overshoot scenarios**

3 Irina Melnikova^{1,2}, Olivier Boucher¹, Patricia Cadule¹, Katsumasa Tanaka^{2,3}, Thomas Gasser⁴,
4 Tomohiro Hajima⁵, Yann Quilcaille⁶, Hideo Shiogama³, Roland Séférian⁷, Kaoru Tachiiri^{3,5},
5 Nicolas Vuichard², Tokuta Yokohata³ and Philippe Ciais²

6 ¹Institut Pierre-Simon Laplace (IPSL), Sorbonne Université / CNRS, Paris, France

7 ²Laboratoire des Sciences du Climat et de l'Environnement (LSCE), IPSL, Commissariat à l'énergie atomique et
8 aux énergies alternatives (CEA/ CNRS/ UVSQ), Université Paris-Saclay, Gif-sur-Yvette, France

9 ³Earth System Division, National Institute for Environmental Studies (NIES), Tsukuba, Japan

10 ⁴International Institute for Applied Systems Analysis (IIASA), Vienna, Austria

11 ⁵Research Institute for Global Change, Japan Agency for Marine-Earth Science and Technology, Kanazawa-ku,
12 Japan

13 ⁶Institute for Atmospheric and Climate Science, ETH Zürich, Switzerland

14 ⁷CNRM, Université de Toulouse, Météo-France, CNRS, Toulouse, France

15 *Correspondence to:* Irina Melnikova (irina.melnikova@lsce.ipsl.fr)

16 **Abstract.** Stringent mitigation pathways frame the deployment of second-generation bioenergy crops combined
17 with Carbon Capture and Storage (CCS) to generate negative CO₂ emissions. This Bioenergy with CCS (BECCS)
18 technology facilitates the achievement of the long-term temperature goal of the Paris Agreement. Here, we use
19 five state-of-the-art Earth System models (ESMs) to explore the consequences of large-scale BECCS deployment
20 on the carbon cycle and carbon-climate feedback under the CMIP6 SSP5-3.4-OS overshoot scenario, keeping in
21 mind that all these models use generic crop vegetation to simulate BECCS crops. We show that an extensive
22 cropland expansion for BECCS causes ecosystem carbon loss that drives the acceleration of carbon turnover and
23 affects the estimates of the absolute values of the global carbon-concentration β and carbon-climate γ feedback
24 parameters. Both parameters decrease so that global β becomes less positive, and γ – more negative. Over the
25 2000–2100 period, the land-use change (LUC) for BECCS leads to an offset of the β -driven carbon uptake by
26 12.2% and amplifies the γ -driven carbon loss by 14.6%. A human choice on land area allocation for energy crops
27 should take into account not only the potential amount of the bioenergy yield but also the LUC emissions, and the
28 associated loss of future potential change in the carbon uptake via the β and γ feedbacks. The dependency of the
29 estimates of β and γ on LUC is very strong after the middle of the 21st century in the SSP5-3.4-OS scenario but it
30 also affects other SSP scenarios and should be taken into account by the integrated assessment modelling teams
31 and accounted for in mitigation policies so as to limit the reductions of the CO₂ fertilization effect where BECCS
32 or land use expansion of short vegetation is applied.



33 **1 Introduction**

34 All stringent future socio-economic mitigation scenarios have negative emissions that rely on carbon dioxide
35 removal (CDR) technologies (Fuss et al., 2014, Rogelj et al., 2018). CDR is important especially in overshoot
36 scenarios, in which temperature temporarily exceeds the given target, e.g., the Paris Agreement temperature target,
37 before ramping down as CO₂ is withdrawn artificially from the atmosphere (Jones et al., 2016a; Keller et al., 2018;
38 Tanaka et al., 2021).

39 Bioenergy with Carbon Capture and Storage (BECCS) is one of the most cost-effective CDR technologies (Jones
40 and Albanito, 2020; Babin et al., 2021). In BECCS, atmospheric CO₂ is captured via photosynthesis and fixed
41 into plant biomass. Harvested biomass is then converted into bioenergy or directly combusted and a fraction of
42 the carbon contained in the CO₂ produced is recuperated and is stored in geological reservoirs without being
43 released back to the atmosphere (Canadell and Schulze, 2014). BECCS is a nascent CDR technology that has not
44 been proven at large spatial scales. Its potential advantages include technical feasibility and a relatively low
45 discounted cost in future decades that allows spreading mitigation efforts over a longer period (Anderson and
46 Peters, 2016; Dooley et al., 2018).

47 The limitations of BECCS are the requirement of potentially large land areas, a loss of biodiversity, and the need
48 for extra water and nutrients (Heck et al., 2018; Séférian et al., 2018; Li et al., 2021). Besides, BECCS may lead
49 to a large amount of carbon emissions from land-use change (LUC), when bioenergy crops are grown over high-
50 carbon content ecosystems such as grassland and forest (Clair et al., 2008; Gibbs et al., 2008; Schueler et al.,
51 2013; Smith et al., 2016; Harper et al., 2018; Whitaker et al., 2018). The LUC emissions released due to land
52 conversion to bioenergy crops include immediate (direct) greenhouse gas (GHG) emissions associated with the
53 destruction of biomass and slash during LUC but also delayed (indirect) emissions from the decay of stumps and
54 soil carbon. These emissions are termed as “carbon debt” (Clair et al., 2008; Fargione et al., 2008; Gibbs et al.,
55 2008; Krause et al., 2018) because for BECCS to be carbon neutral, this loss of carbon must be paid back by
56 several cycles of BECCS harvest followed by carbon geological storage, assumed to substitute with fossil carbon
57 emissions. Using low-productivity marginal or degraded lands for the deployment of second-generation bioenergy
58 crops (such as miscanthus or switchgrass) reduces the carbon debt because such lands have less carbon to lose.
59 Further, soil carbon sequestration, in the long run, may even be achieved with BECCS if non-harvested residues
60 of BECCS crops exceed the carbon input to the soil of the native ecosystems they substitute (Campbell et al.,
61 2008; Gibbs et al., 2008; Mohr and Raman, 2013; Whitaker et al., 2018).

62 The issue with putting second-generation bioenergy crops in low-productivity lands is a need to invest large areas
63 of land (Jones et al., 2016a; Smith et al., 2016). Currently, some land ecosystems act as a carbon sink primarily
64 driven by the CO₂ fertilization effect on photosynthesis and the carbon turnover in ecosystems, which is often
65 expressed as the carbon-concentration (β) feedback, although it is partly counterbalanced by the carbon-climate
66 (γ) feedback (Jones et al., 2016b; Friedlingstein et al., 2020) which expresses the loss of ecosystem carbon per
67 unit of global warming. The β and γ feedback parameters refer to the changes in the ecosystem carbon storage
68 relative to the changes in the atmospheric CO₂ concentration (Δ CO₂) and global surface air temperature (GSAT,
69 Δ T), respectively, relative to the pre-industrial level so that the changes in the carbon storage can be decomposed
70 into the β and γ contributions ($\beta \times \Delta$ CO₂ and $\gamma \times \Delta$ T, respectively). Here the temperature change is taken as a
71 proxy for the response of the ecosystem carbon storage to climate change. As croplands, unlike other ecosystems,
72 have limited potential to store additional carbon because the biomass is harvested regularly, and as the new



73 croplands have a lower soil carbon stock with a short turnover time for soil carbon, the large-scale BECCS
74 deployment must affect the land carbon cycle β and γ feedback parameters, although this has not been specifically
75 looked at in Earth System Models (ESMs) simulation results. Conventionally, β and γ are estimated at a global
76 scale and are assumed to be responses of “natural” ecosystems to the changes in CO_2 and climate, so that the
77 effects of LUC on these parameters are overlooked. No study to date has estimated the effects of BECCS
78 deployment on the terrestrial carbon cycle feedback parameters under overshoot and other scenarios.
79 In this study, we estimate the impact of large-scale BECCS deployment on the carbon cycle feedbacks under the
80 Shared Socioeconomic Pathway (SSP) overshoot scenario named SSP5-3.4-OS that includes mitigation policies
81 via an increase in the land area covered by second-generation bioenergy crops for CDR (Hurtt et al., 2020). We
82 use simulations from five Coupled Model Intercomparison Project 6 (CMIP6) ESMs to decompose the global β
83 and γ contributions to the changes in land carbon pools in ecosystems with and without LUC effects.

84 **2 Data and methods**

85 **2.1 SSP5-3.4-OS scenario**

86 The SSP5-3.4-OS follows the high-emission SSP5-8.5 scenario and branches from it in 2040 when aggressive
87 mitigation policies are implemented (O’Neill et al., 2016; Meinshausen et al., 2020). The delayed mitigation leads
88 to an overshoot of the Paris Agreement 2 °C temperature limit. In addition to a decline in fossil fuel emissions,
89 mitigation efforts after 2040 include the expansion of second-generation bioenergy crops (for BECCS) at the cost
90 mainly of pasture lands (Hurtt et al., 2020). There is no deforestation assumed after 2010, in order to preserve the
91 areas with high carbon content. Second-generation bioenergy crops account for most of the new cropland areas
92 deployed after 2040. In addition, a part of the existing croplands is converted to BECCS (Figure S1).

93 **2.2 CMIP6 ESMs**

94 We use five CMIP6 ESMs that simulate the SSP5-3.4-OS (Table 1). In addition to fully coupled simulations
95 (COU), biogeochemically (BGC) coupled simulations, where only changes in the atmospheric CO_2 concentration,
96 and not the temperature, affect the carbon-cycle processes, are also provided as part of the Coupled Climate–
97 Carbon Cycle Model Intercomparison Project (C4MIP) (Jones et al., 2016b). The combination of COU and BGC
98 simulations allows us to study carbon cycle feedback parameters.

99 The LUC emissions in the ESMs can be estimated as the difference in net biome production (NBP) between
100 simulations with and without land-use change that is between the “historical” and “hist-noLu” simulations for the
101 historical period. However, such simulation pairs for future scenarios such as SSP5-3.4-OS are not usually
102 available. The “fLuc” variable provided by some ESMs enables an alternative way to incompletely quantify direct
103 LUC emissions that include ‘deforestation’ (biomass loss during deforestation), wood harvest, and the release of
104 CO_2 by harvested wood products, but exclude forest regrowth and legacy soil carbon decay or gains. Three
105 models, IPSL-CM6A-LR, CNRM-ESM2-1, and UKESM1-0-LL under consideration, provide the variable “fLuc”
106 (Table 1).

107 Gridded CMIP6 data, with the exception of the “fLuc” variable, were adjusted by subtracting the long-term pre-
108 industrial linear trend from the control (piControl) experiment at a grid level. We used the anomalies relative to



109 the branching year values (indicated in Table S1) for changes in carbon pools and long-term mean piControl
110 values for changes in carbon fluxes.

111 2.3 Methodology

112 ESMs do not provide necessary outputs to diagnose the specific carbon fluxes generated from the transitions to
113 bioenergy crops: 1) they do not treat energy crops explicitly but rather use a generic “crop” vegetation type, itself
114 being a grass with a higher photosynthesis rate in some models, 2) crops only cover a fraction (tile) of a model
115 grid box, and 3) the soil carbon pool is usually not split into tiles for each vegetation type in land surface models.
116 Hence there is no perfect way to diagnose such fluxes. We pragmatically decompose the global β and γ
117 contributions to the changes in land carbon uptake to the contributions that are LUC- and noLUC-induced by
118 using three different approaches described below. In all three considered approaches, the γ feedback parameter is
119 estimated from BGC and COU simulations and not from radiatively coupled (RAD) simulations, where only
120 changes in temperature affect the carbon-cycle processes. First, RAD simulations were not available for the SSP5-
121 3.4-OS pathway. Second, previous studies suggest that using COU and BGC pair for calculating feedback
122 parameters may be more representative because using RAD simulations leads to nonlinearity (non-additivity) of
123 β and γ feedbacks (Jones et al., 2016b; Schwinger and Tjiputra, 2018; Arora et al., 2020).

124 In the “fLuc” approach (1), we exploit the “fLuc” variable provided by most models in CMIP6. We estimate the
125 carbon-concentration β (GtC ppm⁻¹) and carbon-climate γ (GtC °C⁻¹) feedback parameters using BGC and COU
126 simulation outputs as described in previous studies (Friedlingstein et al., 2006; Gregory et al., 2009; Jones et al.,
127 2016; Melnikova et al., 2021):

$$128 \quad \beta = \frac{\Delta C_{BGC}}{\Delta CO_2}, \quad (1)$$

$$129 \quad \gamma = \frac{\Delta C_{COU} - \Delta C_{BGC}}{\Delta T}, \quad (2)$$

130 where ΔC_{BGC} and ΔC_{COU} indicate the changes in the land carbon pool (or cumulative uptake) in BGC and COU
131 simulations, respectively, and ΔCO_2 and ΔT (from COU runs) indicate the changes in the CO₂ concentration and
132 global mean surface air temperature (GSAT), respectively, all reported changes being relative to pre-industrial
133 level (piControl). Because the CO₂ atmospheric concentration is not always reported in the model output, we
134 estimate ΔCO_2 directly from the global CO₂ concentration of input4MIP data set which includes the atmospheric
135 CO₂ concentration pathway used in the concentration-driven simulations (Meinshausen et al., 2020). We
136 performed the calculations using 3-year moving averages.

137 The global carbon flux, NBP that includes changes in ecosystems both with LUC and noLUC effects, cumulated
138 over time, approximates the changes in the land carbon pool. Thus, cumulative NBP + fLuc (because NBP and
139 fLuc have opposite sign conventions with NBP positive sink to land) approximates the changes in the land carbon
140 pool of noLUC ecosystems. Thus, equations (1) and (2) may be transformed to:

$$141 \quad \beta = \beta_{noLUC} - \beta_{LUC}, \quad (3)$$

142 with

$$143 \quad \beta_{noLUC} = \frac{\int NBP_{BGC} dt + \int fLuc_{BGC} dt}{\Delta CO_2}, \quad (4)$$

144 and

$$145 \quad \beta_{LUC} = \frac{\int fLuc_{BGC} dt}{\Delta CO_2}, \quad (5)$$

$$146 \quad \gamma = \gamma_{noLUC} - \gamma_{LUC} \quad (6)$$



147 with

$$148 \gamma_{\text{noLUC}} = \frac{(\int \text{NBP}_{\text{COUdt}} - \int \text{NBP}_{\text{BGCdt}}) + (\int \text{fLUC}_{\text{COUdt}} - \int \text{fLUC}_{\text{BGCdt}})}{\Delta T}, \quad (7)$$

149 and

$$150 \gamma_{\text{LUC}} = \frac{\int \text{fLUC}_{\text{COUdt}} - \int \text{fLUC}_{\text{BGCdt}}}{\Delta T}. \quad (8)$$

151 *In the “cropland threshold” approach (2)*, we divide the global land area into energy-crop-concentrated and
152 no-energy-crop (not energy-crop-concentrated) grid cells by taking into account their evolution after 2015.
153 Hurtt et al. (2020) reported that after 2040, cropland areas expanded “mainly due to large-scale deployment
154 of second-generation bioenergy crops”. We carry out a sensitivity study (Text A1) to label the given grid
155 cell as crop-concentrated if the cropland fraction of the grid cell is larger than a given threshold. In the
156 sensitivity analysis, we examine a range of post-2015 cropland fraction thresholds of the grid box area and
157 select the thresholds that best approximate the total cropland area change in 2015–2100 diagnosed by each
158 ESM. Then, we estimate areal β and γ by using equations (1) and (2) over the energy-crop-concentrated and
159 no-energy-crop areas. Under this approach, the treatment of LUC and noLUC lands and the attribution of
160 the LUC effects on the carbon cycle feedback parameters that are relevant to BECCS are both spatially
161 explicit. The disadvantage of this approach is that by sampling an arbitrary fraction of crop-concentrated
162 grid-cells, we inevitably omit some carbon changes in cropland or encroach carbon belonging to non-crop
163 vegetation.

164 *In the “two simulations” approach (3)*, we performed additional SSP5-3.4-OS scenario simulations by IPSL-
165 CM6A-LR and MIROC-ES2L. In addition to standard SSP5-3.4-OS and SSP5-3.4-OS-BGC simulations,
166 we performed simulations in which land use is held constant corresponding to the 1850 usage (SSP5-3.4-
167 OS-noLUC1850 and SSP5-3.4-OS-noLUC1850-BGC). In addition, using IPSL-CM6A-LR, we performed
168 simulations with 2040 land cover usage (SSP5-3.4-OS-noLUC2040 and SSP5-3.4-OS-noLUC2040-BGC).
169 The difference in NBP between simulations with and without LUC indicates LUC emissions, which are
170 dominated by bioenergy crops area expansion after 2040. The β_{LUC} and γ_{LUC} are estimated as the difference
171 in β and γ contributions, respectively, between two sets of simulations. Unlike in approaches (1) and (2), the
172 term LUC here incorporates a carbon source called the “loss of additional sink capacity” (LASC) relative to
173 the reference years 1850 and 2040 (Gasser and Ciais, 2013; Pongratz et al., 2014). LASC is a change in
174 carbon flux, or a foregone sink, in response to environmental changes on managed land compared to potential
175 natural vegetation. The approach (3) accounts for the indirect LUC emissions while the approaches (1) and
176 (2) do not.

177 3 Evaluation and data consistency

178 The SSP5-3.4-OS is a concentration-driven scenario based on the implementation of SSP5 in the REMIND-
179 MAgPIE (Kriegler et al., 2017; Meinshausen et al., 2020). Bauer et al. (2017), Popp et al. (2017), and Riahi et al.
180 (2017) provide the quantifications, including changes in energy and land use, for the scenario by the IAM. Hurtt
181 et al. (2020) provided the changes in land use in a coherent gridded format required for ESMs in the Harmonization
182 of Global Land-Use Change and Management version 2 (LUH2) project. In LUH2, the historical data (up to the
183 year 2014) based on the History of the Global Environment database (HYDE) and future scenarios (2015–2300)



184 based on IAM are harmonized to minimize the differences between the end of historical reconstruction and IAM
185 initial conditions (Hurtt et al., 2020). The harmonization process, however, is expected to result in some
186 mismatches between LUH2 and the IAM during the early stage of the post-2014 period. First, we check the
187 consistency of the global and regional cropland and other land-state areas reported by REMIND-MAgPIE, LUH2,
188 and CMIP6 ESMs. Second, we evaluate global and regional historical LUC estimates by CMIP6 ESMs against
189 three bookkeeping approaches.

190 **3.1 Consistency of cropland area between REMIND-MAgPIE, LUH2, and ESMs**

191 Under the SSP5-3.4-OS pathway, the cropland area increases by 50% from the 2010 level in the 21st century, so
192 that it reaches 8.1×10^6 km² in 2100 (Hurtt et al., 2020). The global cropland area modelled by REMIND-MAgPIE
193 and downscaled by LUH2 increases due to the expansion of second-generation bioenergy crops. The global
194 cropland areas by REMIND-MAgPIE and LUH2 are largely consistent with a slightly larger area of crops by
195 REMIND-MAgPIE till the 2050s (reaching 0.6×10^6 km² in the year 2050) and a larger area of crops by LUH2
196 in 2060 – 2090s (Figure S2). Unlike in the REMIND-MAgPIE, LUH2 simulates a slight reduction of forest area
197 (by 1.3×10^6 km² in 2100 from 2010 level). The differences in the global cropland area between LUH2 and
198 REMIND-MAgPIE reach 2.9×10^6 km² in the year 2060 that is 14% of the total cropland area of 20.7×10^6 km²
199 by LUH2 in 2060 (and corresponds to a 43.4% increase from the 2015 level) and may cause additional uncertainty
200 in estimates of the BECCS area and LUC. Further, ESMs implement the global and regional gridded cropland
201 fractions following LUH2 and using their own land cover map (Figure S2), with an exception of UKESM1-0-LL
202 that reports an evolution of the global cropland area smaller than those of other ESMs. This deviation of UKESM1-
203 0-LL may occur because of its specifications in the treatment of croplands and the model's dry bias (precipitation
204 deficit) in India and the Sahel (Sellar et al., 2019). While the model used the LUH2 data to prescribe an area
205 available for crops to grow in, this area will be covered by the crop PFTs only if the model's climate is suitable
206 for the grass PFTs, otherwise, the area will remain bare soil.

207 Aside from the deviations in total areas of land cover types between REMIND-MAgPIE, LUH2, and ESMs listed
208 above, a discrepancy arises from the implementation of LUH2's land cover types to the ESM's plant functional
209 types (PFTs). Nevertheless, most CMIP6 ESMs produce croplands area consistent with LUH2. However, the other
210 vegetation classes of LUH2 (e.g., forested lands, non-forested lands, pastures) do not match the PFTs of ESMs
211 because most ESMs decided to use their own land cover map rather than used the LUH2 one for these ecosystems.
212 First, spatial distributions of vegetation classes are tightly associated with climate and biogeochemical processes,
213 and thus, the replacement of the vegetation covers in ESMs would lead to large changes in the model
214 performances. Second, some models that include dynamic vegetation, like UKESM1-0-LL, predict the vegetation
215 distribution change, and sometimes the predicted distribution does not coincide with the real one. Besides, the
216 pastures of REMIND-MAgPIE are translated to two land-use states in LUH2: pastures, and rangelands. While
217 they are treated predominantly as low-productivity areas in REMIND-MAgPIE, this may not be a case in ESMs,
218 where pastures and rangelands may correspond to grasslands and perhaps to shrublands (if this land cover exists
219 in an ESM). We shed light on an issue of inconsistency when translating LUC from IAMs into LUH2 and, then,
220 into ESMs. Overall, implementation of the LUC scenario of REMIND-MAgPIE to first, LUH2, and then ESMs
221 leads to a consistency loss of simulated scenario. This problem requires thorough attention in a separate study.



222 3.2 Evaluation of land-use change emissions

223 The global and regional LUC emissions estimated by ESMs were evaluated against three bookkeeping models for
224 the historical period, namely BLUE (Hansis et al., 2015), HN2017 (Houghton and Nassikas, 2017), and OSCAR
225 (Gasser et al., 2020). The models differ in the spatial units (spatially explicit, country level, region level),
226 parametrization, and process representations (Friedlingstein et al., 2020; Gasser et al., 2020). Unlike other
227 bookkeeping models, OSCAR also reported LASC in LUC estimates but the utilized version did not include peat
228 emissions.

229 Unlike the difference in NBP between simulations with and without LUC, the “fLuc” variable accounts only for
230 the direct LUC emissions and does not account for all the fluxes reported by bookkeeping models, e.g., forest
231 regrowth and slash and soil organic matter decay, as well as for shifting cultivation and degradation (Houghton
232 and Nassikas, 2017). Thus, its values are expected to be lower. We use an average of multiple realizations when
233 provided by the model teams (details in Table S1). The evaluation targets estimating LUC emissions in “fLuc”
234 and “two simulations” approaches.

235 We found that ESMs tend to estimate lower global LUC emissions than bookkeeping models by both “fLuc”
236 variable and “two simulations” approaches (Figure 1). This is remarkable in the three tropical regions that
237 dominate global LUC emissions since the 1960s, and particularly South and Southeast Asia (Figure S3). In 1960–
238 2014, on average, bookkeeping models estimate that three tropical regions account for $56.8 \pm 2.3\%$ of global LUC
239 emissions, while ESMs estimate that they account for $35 \pm 10\%$ based on simulations with and without LUC and
240 $40 \pm 15\%$ based on the “fLUC” variable.

241 LUC emission estimates by MIROC-ES2L (for which only LUC emissions derived from simulations with and
242 without LUC were available) are the most consistent with the estimates of bookkeeping models among considered
243 ESMs (see also Liddicoat et al (2021)). We excluded the estimates of LUC emissions by CNRM-ESM2-1 based
244 on simulations with and without LUC and by UKESM1-0-LL based on “fLuc” from the analysis. CNRM-ESM2-
245 1 estimates much lower LUC emissions derived from simulations with and without LUC than other ESMs,
246 possibly because the CMIP6 version of the model does not include a harvest module, i.e., cropland is modelled as
247 a natural grassland (Séférian et al., 2019) and cropland soils continue to be loaded by harvest inputs. UKESM1-
248 0-LL estimates implausibly low LUC emissions derived from the “fLuc” variable.

249 The LUC emissions estimated by the two approaches differ remarkably due to inconsistent “fLuc” definitions
250 among models (Gasser and Ciais, 2013). We call for a clearer and more rigorous definition of this variable in
251 future MIPs so that model outputs can be compared on the same basis. As some examples for improvement, we
252 suggest that model teams provide variables contained within “fLuc”, e.g., direct deforestation and wood harvest
253 emissions, decomposition flux, as well as indirect emissions, e.g., per each PFT.

254 3.3 Evaluation of land-use change emissions from BECCS deployment

255 BECCS dominates negative emissions in the SSP5-3.4-OS pathway. We confirmed that BECCS is predominantly
256 deployed in low-carbon uptake areas by comparing the changes in carbon pools and NBP globally and crop-
257 concentrated areas (Figure S4). Because bioenergy crops are deployed in low-carbon uptake areas and they
258 dominate LUC emissions in the 21st century, the NBP over crop-concentrated areas derived by the “cropland
259 threshold” approach approximates global LUC emissions (Figure S5). The comparison of NBP in crop-
260 concentrated grids with the original LUC emissions of the REMIND-MAGPIE IAM scenario confirms a similar



261 trend between IAM-based global LUC emissions and ESMs-based global temporal NBP changes in the crop-
262 concentrated areas after 2040. The strong correlation is evident in three ESMs, namely CanESM5, UKESM1-0-
263 LL, and MIROC-ES2L (correlation coefficient is 0.72 for the 2015–2100 period). The carbon loss in the crop-
264 concentrated areas over the 21st century period averaged over these three ESMs reaches 37.8 ± 30.3 GtC. Two
265 models, IPSL-CM6A-LR and CNRM-ESM2-1, however, do not capture the increased carbon loss after 2040
266 perhaps due to low estimates of LUC emissions from crop expansion (especially, CNRM-ESM2-1) or
267 overestimated uptake by no-LUC areas (Figures 1, S3). Besides, IPSL-CM6A-LR simulates the lowest ecosystem
268 carbon pool, especially in soils (Figure S6) that may lead to relatively small LUC-induced carbon losses when
269 cropland areas expand. Thus, the estimates of LUC impact on carbon cycle feedbacks from IPSL-CM6A-LR and
270 CNRM-ESM2-1 need to be considered with the above-mentioned caveats.

271 **4 The impact of LUC on the carbon cycle feedback parameters**

272 **4.1 Differences in LUC impact on carbon cycle estimated by three approaches**

273 We use the estimates of the LUC impacts on global β and γ by IPSL-CM6A-LR and MIROC-ES2L to compare
274 the three approaches described in sect. 2.3 between each other. The “cropland threshold”, unlike the other two
275 approaches, separates cropland-concentrated and no-crop contributions spatially. Thus, the estimated carbon cycle
276 feedback parameters are areal cumulative. In the other two approaches, in contrast, the β and γ are calculated in
277 each grid cell for both LUC-dominated and noLUC ecosystems, so that carbon change of these two land-use
278 categories may partly offset each other. For this reason, the carbon cycle feedback parameters, especially β ,
279 estimated via “cropland threshold” are of smaller magnitudes (sometimes by several times) than those estimated
280 via the “two simulations since 1850” approach (Figure 2). A larger loss is seen in “two simulations since 1850”
281 because these simulations include LASC and legacy soil emissions (Figure 2a). Intermediate loss is from “fLUC”
282 because this approach includes only immediate (direct) carbon loss. Lower carbon losses correspond to “cropland
283 threshold” that also includes a carbon sink in natural ecosystems over selected grid cells and misses initial carbon
284 loss, and to “two simulations since 2040” that misses legacy emissions of activities before 2040. The larger carbon
285 losses in “two simulations since 1850” than in “two simulations since 2040” also reveal the long-term effects of
286 LUC.

287 In the case of IPSL-CM6A-LR, the “fLuc” and “two simulations” approaches suggest that a BECCS-related
288 carbon loss leads to a negative β_{LUC} , and the “cropland threshold” and “two simulations” approaches suggest that
289 a carbon loss and climate effects on enhancing soil carbon decomposition leads to a negative γ_{LUC} . The “cropland
290 threshold” and “two simulations since 2040” approaches produce similar estimates of LUC impact on cumulative
291 β and γ contributions to land carbon because these two methods target the changes in the carbon fluxes particularly
292 due to cropland expansion for BECCS in the 21st century (Figure 2). MIROC-ES2L that account for gross LUC
293 emissions (Liddicoat et al., 2021) produce similar estimates of LUC impact by “cropland threshold” and “two
294 simulations since 1850” approaches (except for differences in β explained above).

295 **4.2 Temporal impacts of LUC on global β and γ**

296 Figure 3 illustrates the attribution of global β - and γ -driven carbon fluxes to LUC- (or crop-concentrated) and no-
297 LUC (no-crop) ecosystems by five ESMs and three approaches. They show that the large-scale deployment of



298 bioenergy crops even on low carbon-uptake areas causes a carbon loss from the ecosystem and alters carbon cycle
299 feedback parameters.

300 For the “cropland threshold” approach, the majority of ESM simulations, excluding IPSL-CM6A-LR and CNRM-
301 ESM2-1 (see section 3.3), agree that cropland expansion causes a decrease in global β and that β is negative in
302 crop-concentrated grids which lose carbon from LUC (Figure 3, Table S2). Cropland expansion for BECCS may
303 also contribute to the global γ change towards more negative values (larger carbon source). However, these
304 changes are small in the “cropland threshold” and absent in “fLUC” estimates. We speculate this occurs because
305 the “fLUC” variable involves only direct LUC changes such as deforestation, wood harvest, and soil carbon decay.
306 On top of it, earlier findings show that the ESMs misrepresent the amplitude and rate of changes in soil and litter
307 carbon after LUC (Brovkin et al., 2021).

308 The γ estimates are in less agreement between ESMs than β , and they are more uncertain when estimated from
309 BGC and COU simulations, as opposed to RAD runs (Schwinger and Tjiputra, 2018). The LUC carbon losses for
310 BECCS deployment cannot be overridden by the increased CO₂ effects (Figure S7). This causes a decrease in the
311 global β feedback parameter. Although more studies are needed to confirm the impacts of BECCS-associated
312 LUC carbon losses on the global γ , the majority of simulations confirm a contribution of LUC ecosystems to the
313 negative γ . Overall, the three approaches and five ESMs demonstrate that the BECCS expansion under the SSP5-
314 3.4-OS pathway results in 42.55 ± 41.08 GtC loss that corresponds to 12.2% of noLUC β -driven uptake and to an
315 additional 13.00 ± 12.27 GtC loss that corresponds to 14.6% of noLUC γ -driven loss over the 2000–2100 period
316 (Tables S2, S3).

317 **4.3 Spatial variation of impacts of LUC on global β and γ**

318 The spatial variation of β and γ differs among ESMs but the majority agrees on the globally positive β with larger
319 magnitude in the low latitudes and on the positive and negative γ in the northern high latitudes and low latitudes,
320 respectively (Figures 4, S8).

321 The carbon cycle feedback parameters are expected to increase after the peak of CO₂ concentration and
322 temperature. Melnikova et al. (2021) reported that in the SSP5-3.4-OS scenario, the global β and γ parameters
323 continue to increase even after the peaks of CO₂ concentration and temperature at least till the end of the 21st
324 century due to the inertia of the Earth system. After the start of BECCS deployment, the β parameter increases
325 globally except for the BECCS areas, especially in the tropical region, where it becomes negative (Figure 4).
326 These differences are apparent in CanESM5, UKESM1-0-LL, and MIROC-ES2L. The positive γ parameter
327 increases in the high latitudes except for the areas of the eastern part of North America and part of Europe almost
328 exactly in the areas of BECCS deployment, where the γ is zero or negative (Figure S8). The increase in negative
329 γ over low-latitudes occurs both in the areas with and without the presence of BECCS. Even though the SSP5-
330 3.4-OS scenario is designed so that BECCS utilizes low carbon areas to cause the least possible impact on the
331 carbon sink in unmanaged lands, these BECCS areas lose their β -driven carbon uptake potential but do not escape
332 γ -driven carbon losses. The spatial variation of β and γ in simulation with and without LUC by MIROC-ES2L
333 and IPSL-CM6A-LR also demonstrates a decrease in positive β and to a lesser scale an increase in negative γ over
334 BECCS areas (Figure S9).

335 We explored the drivers of the β - and γ -driven carbon losses by analysing the changes in the spatial distribution
336 of ecosystem carbon turnover time τ_{eco} defined as the ratio of land carbon stock to net primary production (NPP).



337 Previous studies demonstrated that land-use change is a major driver of τ_{eco} decrease (Wu et al., 2020; Erb et al.,
338 2016). We found that the majority of ESMs (with an exception of CNRM-ESM2-1) show an acceleration of carbon
339 turnover in the areas of BECCS deployment due to LUC-driven ecosystem carbon loss (Figure S10 a-c). The
340 carbon cycle feedback parameters are directly correlated with τ_{eco} over the areas of BECCS deployment, which is
341 apparent in CanESM5, UKESM1-0-LL, and MIROC-ES2L (Figure S10 d, e). LUC causes an ecosystem carbon
342 loss that drives the acceleration of carbon turnover and results in alteration of β and γ feedback parameters.
343 The β and γ feedback parameters are assumed to be a pure response to the CO_2 concentration and temperature
344 changes. However, they are also a function of the land cover. In the SSP5-3.4-OS scenario, second-generation
345 biofuel cropland areas estimated by LUH2 reach nearly 6% of global land (potentially vegetated) area in 2100.
346 Assigning such vast areas to bioenergy crops - even if they correspond to low-carbon content ecosystems - affects
347 the land carbon uptake and the global carbon cycle feedback parameters. The decision on the assignment of these
348 areas for energy crops requires assessment of both the current state of the ecosystem, e.g., the carbon content in
349 vegetation and soil, and the future potential increase in the carbon uptake via the β and γ feedbacks. The
350 dependency of global β and γ on LUC should be accounted for in developing future mitigation pathways so that
351 the benefits of BECCS are not minimized by adverse modulations of carbon cycle feedback parameters.

352 5 Conclusion

353 In this study, we investigated the impacts of BECCS deployment on the carbon-concentration β and carbon-
354 climate γ feedback parameters under an overshoot pathway. In a broader sense, the land-cover and land-use
355 associated differences in the initial conditions of ESMs simulations may influence the estimates of global carbon
356 cycle feedback parameters even under the idealized pathways. The divergences in the pre-industrial land covers
357 among ESMs lead to spatial differences in the ecosystem carbon stocks (e.g., ESM with larger forest cover has
358 larger land carbon pool size). Furthermore, the pre-industrial levels of ecosystem carbon stock vary among models
359 even for identical land-cover types. The estimated global β and γ feedbacks compromise these land-cover-related
360 uncertainties. While the β and γ are often compared between ESMs in idealized scenarios (such as 1% CO_2
361 increase), the land-cover impacts have not been discussed. Future studies should address the issue by
362 benchmarking the sets of idealized experiments with different types of land-cover and land-use changes.

363 In the evaluation part of this study, we highlighted some inconsistencies in the land-use states and their temporal
364 transitions between the REMIND-MAgPIE, LUH2, and ESMs. While differences in LUC may arise from
365 differences in process representations across models and initial conditions, we emphasize that the inconsistencies
366 should be taken into account in comparative studies of IAMs and ESMs. Further work will be required to address
367 the issue of the level of inconsistency between the IAMs, LUH2, and ESMs that should be tolerated to have
368 confidence that ESMs and IAMs describe the same scenario.

369 We exploit five ESMs and three approaches to show that cropland expansion for BECCS causes a carbon loss
370 even in low-carbon uptake lands and reduces the future potential increase in the global carbon uptake via LUC
371 impact on the carbon-concentration and carbon-climate feedbacks. Under the SSP5-3.4-OS, the LUC emissions
372 from BECCS deployment cause a decrease in global β and contribute to negative γ feedback parameter. The fact
373 that the impact on β dominates that on γ , which probably reflects the larger role of β -driven carbon uptake than
374 that of γ -driven loss in the current world and under overshoot pathways (of moderate level).



375 Our results are consistent with IPCC special report on climate change and land (Shukla et al., 2019) and highlight
376 the need for considering trade-offs in BECCS deployment and other land-uses but, to some extent, they go beyond
377 this assessment by considering the implication of carbon cycle feedbacks. Our work shows that areas best suited
378 for BECCS should also be assessed both in terms of their potential amount of the bioenergy yield and potential
379 future impact on the β and γ feedback parameters. Future studies need to further investigate the potential of
380 BECCS to provide negative carbon emissions with little loss of storage from the β and γ feedbacks.

381 **Data availability**

382 The data from the CMIP6 simulations are available from the CMIP6 archive ([https://esgf-](https://esgf-node.llnl.gov/search/cmip6)
383 [node.llnl.gov/search/cmip6](https://esgf-node.llnl.gov/search/cmip6)), the LUH2 data from <https://luh.umd.edu/data.shtml>, and the IIASA database via
384 <https://tntcat.iiasa.ac.at/SspDb/dsd?Action=htmlpage&page=welcome>. We obtained LUC emission data of
385 bookkeeping approaches from the modelling teams and <https://dare.iiasa.ac.at/103/> for OSCAR.

386 **Author Contributions**

387 O.B., P.Ciais, K.Tanaka, and I.M. initiated the study, all co-authors provided input into developing the study
388 ideas. I.M. performed data analysis and wrote the initial draft. T.H. (MIROC-ES2L) and P.Cadule (IPSL-CM6A-
389 LR) performed additional ESM simulations. All authors contributed to writing and commenting on the paper.

390 **Competing Interests**

391 The authors have the following competing interests: Roland Séférian is editor of ESD.

392 **Acknowledgments**

393 We acknowledge the World Climate Research Programme, which, through its Working Group on Coupled
394 Modelling, coordinated and promoted CMIP6. We thank the climate modelling groups for producing and making
395 available their model output, the Earth System Grid Federation (ESGF) for archiving the data and providing
396 access, and the multiple funding agencies who support CMIP6 and ESGF. We thank Richard Houghton of
397 Woodwell Climate Research Center for providing the regional annual fluxes for LUC from HN2017, Eddy
398 Robertson of Met Office, Vivek Arora of Canadian Centre for Climate Modelling and Analysis for providing
399 additional information on the LUC implementation in ESMs. The IPSL-CM6 experiments were performed using
400 the HPC resources of TGCC under the allocation 2020-A0080107732 (project gencmip6) provided by GENCI
401 (Grand Equipement National de Calcul Intensif). This study benefited from State assistance managed by the
402 National Research Agency in France under the Programme d'Investissements d'Avenir under the reference ANR-
403 19-MPGA-0008. Our study was also supported by the European Union's Horizon 2020 research and innovation
404 programme under grant agreement number 820829 for the "Constraining uncertainty of multi-decadal climate
405 projections (CONSTRAIN)" project, by a grant from the French Ministry of the Ecological Transition as part of
406 the Convention on financial support for climate services, by the Ministry of Education, Culture, Sports, Science
407 and Technology (MEXT) of Japan (Integrated Research Program for Advancing Climate Models, grant no.



408 JPMXD0717935715) and the Environment Research and Technology Development Fund (JPMEERF20192004)
409 of the Environmental Restoration and Conservation Agency of Japan. RS acknowledges the European Union's
410 Horizon 2020 research and innovation programme under grant agreement No 101003536 (ESM2025 – Earth
411 System Models for the Future). RS acknowledges the support of the team in charge of the CNRM-CM climate
412 model. Supercomputing time was provided by the Météo-France/DSI supercomputing center.
413

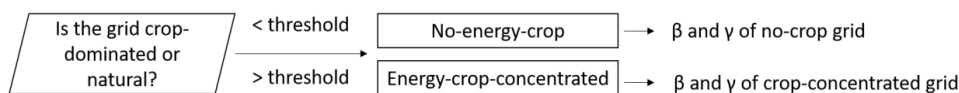


414 **Appendix**

415 **Text A1. Sensitivity study for deriving the crop-concentrated grid thresholds**

416 Neither IAMs nor ESMs provide BECCS-related LUC emissions. Separating BECCS-related emissions from all
417 other LUC emissions is virtually impossible due to spatial heterogeneity and many complex factors that affect the
418 bioenergy crop deployment.

419 ESMs do not distinguish second-generation bioenergy crops from other crops in CMIP6. Moreover, the cropland
420 area in ESMs is defined at a sub-grid scale (i.e., on a fraction or tile of a grid box). Because land-use states (e.g.,
421 forest, crops, pastures) vary in productivity and, thus, carbon uptakes and because modelling teams do not provide
422 NBP estimates at the sub-grid level, to estimate the area and carbon fluxes of the biofuel crops in ESMs, we
423 assume that all croplands deployed after the 2040s are for second-generation biofuel crops (Figure A1). We label
424 the given grid of CMIP6 simulation outputs as crop-concentrated if the cropland fraction of the grid is larger than
425 a given threshold derived via a sensitivity analysis (Figure A1).

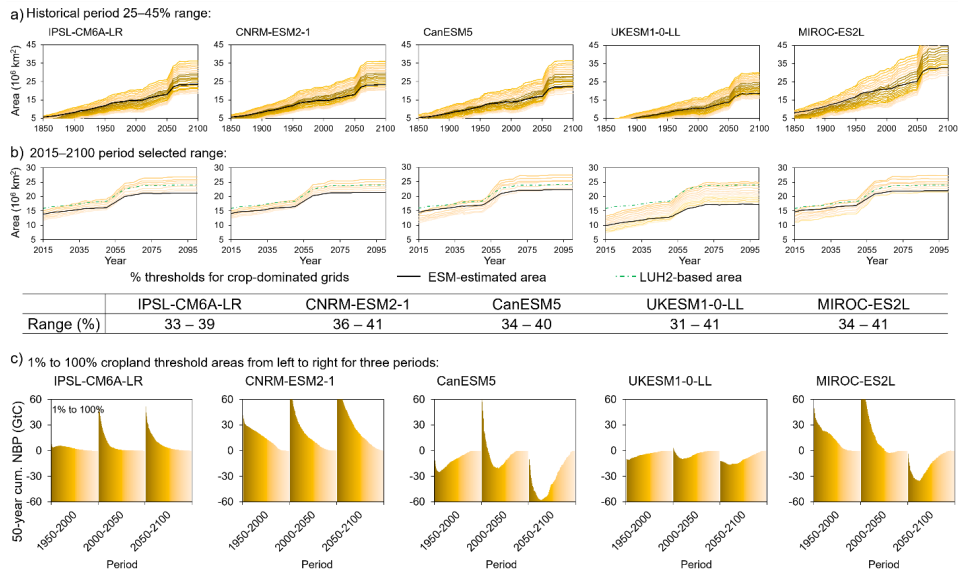


426

427 **Figure A1: A schematic presentation of the sensitivity study for estimating the carbon-climate feedback parameters**
428 **over the energy-crop-concentrated and no-energy-crop grids.**

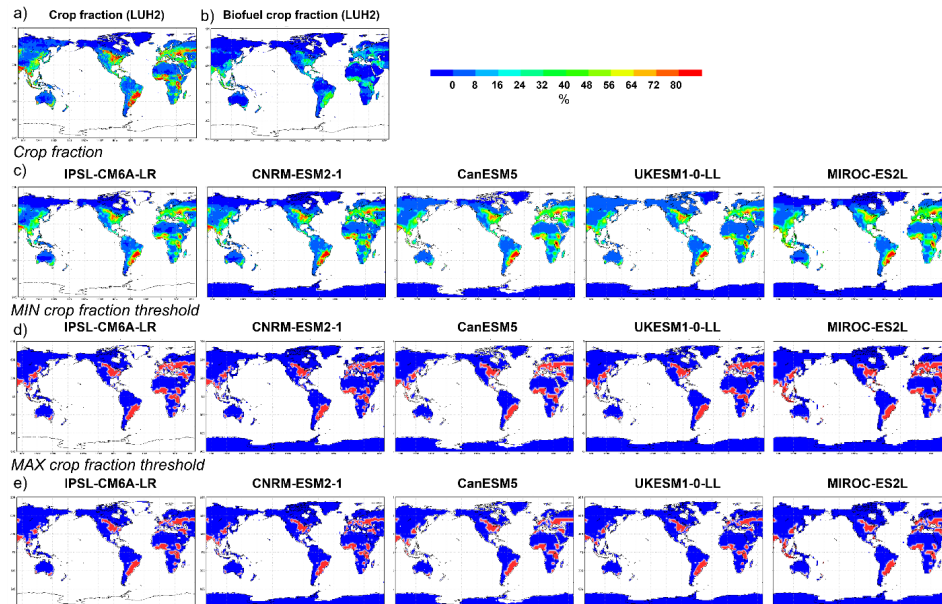
429 We examined time-invariant cropland fraction thresholds ranging from 25% to 45% of the grid box area and
430 selected a range of thresholds that best approximate the change in the total cropland area of each ESM in 2015–
431 2100 (Figure A2). Here we choose the fitting period of 2015 – 2100 because a shorter period (2040–2100) would
432 result in a lower threshold during the 2050 – 2060 period with a large global cropland increase. More specifically,
433 we selected a range of thresholds with a 1%-step so that they intersect at least once either the global cropland area
434 estimated by ESM itself or LUH2 data set from 2015 to 2100. Although, the selected ensembles of thresholds are
435 time-invariant, the resultant cropland area increases. We find that for a later period (end of the 21st century), a
436 higher threshold is required because both the spatial coverage (the number of grid boxes that have crops) and
437 cropland concentration (a grid fraction of cropland) increases (Figure A2).

438 We confirmed the spatial distribution of the minimum and maximum selected thresholds of energy-crop-
439 concentrated grids against sub-grid scale ESM and the LUH2 estimates of cropland area (Figure A3).



440

441 **Figure A2:** (a) The cropland-fraction thresholds ranging from 25% to 45% of the grid box area analyzed in the
 442 sensitivity study and (b) the selected (resultant) range of thresholds for identifying the energy-crop-concentrated area
 443 with the selected range for each ESM indicated in the table. Panel (c) shows the cumulative NBP of the areas
 444 corresponding to the range of cropland thresholds from 1 to 100% (left dark to right light color) in three periods.



445 **Figure A3:** Spatial variation of (a) grid cropland fraction (b) and second-generation bioenergy cropland fraction by
 446 LUH2. Panel (c) shows the spatial variation of grid cropland fraction estimated by CMIP6 ESMs. The spatial variation
 447 of the selected (d) minimum and (e) maximum thresholds (that intersect at least once either the global cropland area
 448 estimated by ESM itself or LUH2 data set from 2015 to 2100 as shown in Figure A1) for estimating crop-concentrated
 449 grids in 2100.

451



452 **References**

- 453 Anderson, K. and Peters, G.: The trouble with negative emissions, *Science*, 354, 182,
454 <https://doi.org/10.1126/science.aah4567>, 2016.
- 455 Arora, V. K., Katavouta, A., Williams, R. G., Jones, C. D., Brovkin, V., Friedlingstein, P., Schwinger, J., Bopp,
456 L., Boucher, O., Cadule, P., Chamberlain, M. A., Christian, J. R., Delire, C., Fisher, R. A., Hajima, T., Ilyina, T.,
457 Joetzjer, E., Kawamiya, M., Koven, C. D., Krasting, J. P., Law, R. M., Lawrence, D. M., Lenton, A., Lindsay, K.,
458 Pongratz, J., Raddatz, T., Séférian, R., Tachiiri, K., Tjiputra, J. F., Wiltshire, A., Wu, T., and Ziehn, T.: Carbon-
459 concentration and carbon–climate feedbacks in CMIP6 models and their comparison to CMIP5 models,
460 *Biogeosciences*, 17, 4173–4222, <https://doi.org/10.5194/bg-17-4173-2020>, 2020.
- 461 Babin, A., Vaneekhaute, C., and Iliuta, M. C.: Potential and challenges of bioenergy with carbon capture and
462 storage as a carbon-negative energy source: A review, *Biomass and Bioenergy*, 146, 105968,
463 <https://doi.org/10.1016/j.biombioe.2021.105968>, 2021.
- 464 Bauer, N., Calvin, K., Emmerling, J., Fricko, O., Fujimori, S., Hilaire, J., Eom, J., Krey, V., Kriegler, E.,
465 Mouratiadou, I., de Boer, H. S., van den Berg, M., Carrara, S., Daioglou, V., Drouet, L., Edmonds, J. E., Gernaat,
466 D., Havlik, P., Johnson, N., Klein, D., Kyle, P., Marangoni, G., Masui, T., Pietzcker, R. C., Strubegger, M., Wise,
467 M., Riahi, K., and van Vuuren, D. P.: Shared Socio-Economic Pathways of the Energy Sector – Quantifying the
468 Narratives, *Glob. Environ. Change*, 42, 316–330, <https://doi.org/10.1016/j.gloenvcha.2016.07.006>, 2017.
- 469 Boucher, O., Servonnat, J., Albright, A. L., Aumont, O., Balkanski, Y., Bastrikov, V., Bekki, S., Bonnet, R., Bony,
470 S., Bopp, L., Braconnot, P., Brockmann, P., Cadule, P., Caubel, A., Cheruy, F., Codron, F., Cozic, A., Cugnet,
471 D., D’Andrea, F., Davini, P., Lavergne, C. de, Denvil, S., Deshayes, J., Devilliers, M., Ducharne, A., Dufresne,
472 J.-L., Dupont, E., Éthé, C., Fairhead, L., Falletti, L., Flavoni, S., Foujols, M.-A., Gardoll, S., Gastineau, G.,
473 Ghattas, J., Grandpeix, J.-Y., Guenet, B., Guez, L., E., Guilyardi, E., Guimberteau, M., Hauglustaine, D., Hourdin,
474 F., Idelkadi, A., Joussaume, S., Kageyama, M., Khodri, M., Krinner, G., Lebas, N., Levvasseur, G., Lévy, C., Li,
475 L., Lott, F., Lurton, T., Luyssaert, S., Madec, G., Madeleine, J.-B., Maignan, F., Marchand, M., Marti, O., Mellul,
476 L., Meurdesoif, Y., Mignot, J., Musat, I., Ottlé, C., Peylin, P., Planton, Y., Polcher, J., Rio, C., Rochetin, N.,
477 Rousset, C., Sepulchre, P., Sima, A., Swingedouw, D., Thiéblemont, R., Traore, A. K., Vancoppenolle, M., Vial,
478 J., Vialard, J., Viovy, N., and Vuichard, N.: Presentation and Evaluation of the IPSL-CM6A-LR Climate Model,
479 *J. Adv. Model Earth Sy.*, 12, e2019MS002010, <https://doi.org/10.1029/2019MS002010>, 2020.
- 480 Brovkin, V., Boysen, L., Wärlind, D., Peano, D., Lansø, A. S., Delire, C., Burke, E., Poeplau, C., and Don, A.:
481 Evaluation of soil carbon dynamics after land use change in CMIP6 land models using chronosequences, EGU
482 General Assembly 2021, online, 19–30 Apr 2021, EGU21-12561, <https://doi.org/10.5194/egusphere-egu21-12561>, 2021. Campbell, J. E., Lobell, D. B., Genova, R. C., and Field, C. B.: The global potential of bioenergy
483 on abandoned agriculture lands, *Environ Sci Technol.*, 42, 5791–5794, <https://doi.org/10.1021/es800052w>, 2008.
- 485 Canadell, J. G. and Schulze, E. D.: Global potential of biospheric carbon management for climate mitigation, *Nat.*
486 *Commun.*, 5, 1–12, <https://doi.org/10.1038/ncomms6282>, 2014.
- 487 Clair, S. S., Hillier, J., and Smith, P.: Estimating the pre-harvest greenhouse gas costs of energy crop production,
488 *Biomass Bioenerg.*, 32, 442–452, <https://doi.org/10.1016/j.biombioe.2007.11.001>, 2008.
- 489 Dooley, K., Christoff, P., and Nicholas, K. A.: Co-producing climate policy and negative emissions: trade-offs
490 for sustainable land-use, *Global Sustainability*, 1, <https://doi.org/10.1017/sus.2018.6>, 2018.
- 491 Erb, K.-H., Fetzel, T., Plutzer, C., Kastner, T., Lauk, C., Mayer, A., Niedertscheider, M., Körner, C., and Haberl,
492 H.: Biomass turnover time in terrestrial ecosystems halved by land use, *Nature Geoscience*, 9, 674–678,
493 <https://doi.org/10.1038/ngeo2782>, 2016.
- 494 Fargione, J., Hill, J., Tilman, D., Polasky, S., and Hawthorne, P.: Land Clearing and the Biofuel Carbon Debt,
495 *Science*, 319, 1235, <https://doi.org/10.1126/science.1152747>, 2008.
- 496 Friedlingstein, P., Cox, P., Betts, R., Bopp, L., von Bloh, W., Brovkin, V., Cadule, P., Doney, S., Eby, M., Fung,
497 I., Bala, G., John, J., Jones, C., Joos, F., Kato, T., Kawamiya, M., Knorr, W., Lindsay, K., Matthews, H. D.,
498 Raddatz, T., Rayner, P., Reick, C., Roeckner, E., Schnitzler, K.-G., Schnur, R., Strassmann, K., Weaver, A. J.,



- 499 Yoshikawa, C., and Zeng, N.: Climate–Carbon Cycle Feedback Analysis: Results from the C4MIP Model
500 Intercomparison, *J. Climate*, 19, 3337–3353, <https://doi.org/10.1175/JCLI3800.1>, 2006.
- 501 Friedlingstein, P., O’Sullivan, M., Jones, M. W., Andrew, R. M., Hauck, J., Olsen, A., Peters, G. P., Peters, W.,
502 Pongratz, J., Sitch, S., Le Quééré, C., Canadell, J. G., Ciais, P., Jackson, R. B., Alin, S., Aragão, L. E. O. C., Arneeth,
503 A., Arora, V., Bates, N. R., Becker, M., Benoit-Cattin, A., Bittig, H. C., Bopp, L., Bultan, S., Chandra, N.,
504 Chevallier, F., Chini, L. P., Evans, W., Florentie, L., Forster, P. M., Gasser, T., Gehlen, M., Gilfillan, D.,
505 Gkritzalis, T., Gregor, L., Gruber, N., Harris, I., Hartung, K., Haverd, V., Houghton, R. A., Ilyina, T., Jain, A. K.,
506 Joetzier, E., Kadono, K., Kato, E., Kitidis, V., Korsbakken, J. I., Landschützer, P., Lefèvre, N., Lenton, A., Lienert,
507 S., Liu, Z., Lombardozzi, D., Marland, G., Metzl, N., Munro, D. R., Nabel, J. E. M. S., Nakaoka, S.-I., Niwa, Y.,
508 O’Brien, K., Ono, T., Palmer, P. I., Pierrot, D., Poulter, B., Resplandy, L., Robertson, E., Rödenbeck, C.,
509 Schwinger, J., Séférian, R., Skjelvan, I., Smith, A. J. P., Sutton, A. J., Tanhua, T., Tans, P. P., Tian, H., Tilbrook,
510 B., van der Werf, G., Vuichard, N., Walker, A. P., Wanninkhof, R., Watson, A. J., Willis, D., Wiltshire, A. J.,
511 Yuan, W., Yue, X., and Zaehle, S.: Global Carbon Budget 2020, *Earth Syst. Sci. Data*, 12, 3269–3340,
512 <https://doi.org/10.5194/essd-12-3269-2020>, 2020.
- 513 Gasser, T. and Ciais, P.: A theoretical framework for the net land-to-atmosphere CO₂ flux and its implications in
514 the definition of “emissions from land-use change”, *Earth Syst. Dynam.*, 4, 171–186, <https://doi.org/10.5194/esd-4-171-2013>, 2013.
- 516 Gasser, T., Crepin, L., Quilcaille, Y., Houghton, R. A., Ciais, P., and Obersteiner, M.: Historical CO₂ emissions
517 from land use and land cover change and their uncertainty, *Biogeosciences*, 17, 4075–4101,
518 <https://doi.org/10.5194/bg-17-4075-2020>, 2020.
- 519 Gibbs, H. K., Johnston, M., Foley, J. A., Holloway, T., Monfreda, C., Ramankutty, N., and Zaks, D.: Carbon
520 payback times for crop-based biofuel expansion in the tropics: the effects of changing yield and technology,
521 *Environ Res Lett.*, 3, 034001, <https://doi.org/10.1088/1748-9326/3/3/034001>, 2008.
- 522 Gregory, J. M., Jones, C. D., Cadule, P., and Friedlingstein, P.: Quantifying Carbon Cycle Feedbacks, *J. Climate*,
523 22, 5232–5250, <https://doi.org/10.1175/2009JCLI2949.1>, 2009.
- 524 Hajima, T., Watanabe, M., Yamamoto, A., Tabebe, H., Noguchi, M. A., Abe, M., Ohgaito, R., Ito, A., Yamazaki,
525 D., Okajima, H., Ito, A., Takata, K., Ogochi, K., Watanabe, S., and Kawamiya, M.: Development of the MIROC-
526 ES2L Earth system model and the evaluation of biogeochemical processes and feedbacks, *Geosci. Model Dev.*,
527 13, 2197–2244, <https://doi.org/10.5194/gmd-13-2197-2020>, 2020.
- 528 Hansis, E., Davis, S. J., and Pongratz, J.: Relevance of methodological choices for accounting of land use change
529 carbon fluxes, *Global. Biogeochem. Cy.*, 29, 1230–1246, <https://doi.org/10.1002/2014GB004997>, 2015.
- 530 Harper, A. B., Powell, T., Cox, P. M., House, J., Huntingford, C., Lenton, T. M., Sitch, S., Burke, E., Chadburn,
531 S. E., Collins, W. J., Comyn-Platt, E., Daioglou, V., Doelman, J. C., Hayman, G., Robertson, E., van Vuuren, D.,
532 Wiltshire, A., Webber, C. P., Bastos, A., Boysen, L., Ciais, P., Devaraju, N., Jain, A. K., Krause, A., Poulter, B.,
533 and Shu, S.: Land-use emissions play a critical role in land-based mitigation for Paris climate targets, *Nat.*
534 *Commun.*, 9, 2938, <https://doi.org/10.1038/s41467-018-05340-z>, 2018.
- 535 Heck, V., Gerten, D., Lucht, W., and Popp, A.: Biomass-based negative emissions difficult to reconcile with
536 planetary boundaries, *Nat. Clim. Change*, 8, 151–155, <https://doi.org/10.1038/s41558-017-0064-y>, 2018.
- 537 Houghton, R. A. and Nassikas, A. A.: Global and regional fluxes of carbon from land use and land cover change
538 1850–2015, *Global. Biogeochem. Cy.*, 31, 456–472, <https://doi.org/10.1002/2016GB005546>, 2017.
- 539 Hurtt, G. C., Chini, L., Sahajpal, R., Froking, S., Bodirsky, B. L., Calvin, K., Doelman, J. C., Fisk, J., Fujimori,
540 S., Goldewijk, K. K., Hasegawa, T., Havlik, P., Heinemann, A., Humpenöder, F., Jungclaus, J., Kaplan, J.,
541 Kennedy, J., Kristzin, T., Lawrence, D., Lawrence, P., Ma, L., Mertz, O., Pongratz, J., Popp, A., Poulter, B., Riahi,
542 K., Shevliakova, E., Stehfest, E., Thornton, P., Tubiello, F. N., van Vuuren, D. P., and Zhang, X.: Harmonization
543 of Global Land-Use Change and Management for the Period 850-2100 (LUH2) for CMIP6, *Geosci Model Dev.*,
544 1–65, <https://doi.org/10.5194/gmd-2019-360>, 2020.
- 545 Jones, C. D., Arora, V., Friedlingstein, P., Bopp, L., Brovkin, V., Dunne, J., Graven, H., Hoffman, F., Ilyina, T.,
546 John, J. G., Jung, M., Kawamiya, M., Koven, C., Pongratz, J., Raddatz, T., Randerson, J. T., and Zaehle, S.:



- 547 C4MIP - The Coupled Climate–Carbon Cycle Model Intercomparison Project: experimental protocol for CMIP6,
548 Geosci. Model Dev., 9, 2853–2880, <https://doi.org/10.5194/gmd-9-2853-2016>, 2016a.
- 549 Jones, C. D., Ciais, P., Davis, S. J., Friedlingstein, P., Gasser, T., Peters, G. P., Rogelj, J., van Vuuren, D. P.,
550 Canadell, J. G., Cowie, A., Jackson, R. B., Jonas, M., Kriegler, E., Littleton, E., Lowe, J. A., Milne, J., Shrestha,
551 G., Smith, P., Torvanger, A., and Wiltshire, A.: Simulating the Earth system response to negative emissions,
552 Environ. Res. Lett., 11, 095012, <https://doi.org/10.1088/1748-9326/11/9/095012>, 2016b.
- 553 Jones, M. B. and Albanito, F.: Can biomass supply meet the demands of bioenergy with carbon capture and storage
554 (BECCS)?, Glob. Change Biol., 26, 5358–5364, <https://doi.org/10.1111/gcb.15296>, 2020.
- 555 Keller, D. P., Lenton, A., Scott, V., Vaughan, N. E., Bauer, N., Ji, D., Jones, C. D., Kravitz, B., Muri, H., and
556 Zickfeld, K.: The Carbon Dioxide Removal Model Intercomparison Project (CDRMIP): rationale and
557 experimental protocol for CMIP6, Geosci. Model Dev., 11, 1133–1160, <https://doi.org/10.5194/gmd-11-1133-2018>, 2018.
- 559 Krause, A., Pugh, T. A. M., Bayer, A. D., Li, W., Leung, F., Bondeau, A., Doelman, J. C., Humpenöder, F.,
560 Anthoni, P., Bodirsky, B. L., Ciais, P., Müller, C., Murray-Tortarolo, G., Olin, S., Popp, A., Sitch, S., Stehfest,
561 E., and Arneeth, A.: Large uncertainty in carbon uptake potential of land-based climate-change mitigation efforts,
562 Glob. Change Biol., 24, 3025–3038, <https://doi.org/10.1111/gcb.14144>, 2018.
- 563 Kriegler, E., Bauer, N., Popp, A., Humpenöder, F., Leimbach, M., Strefler, J., Baumstark, L., Bodirsky, B. L.,
564 Hilaire, J., Klein, D., Mouratiadou, I., Weindl, I., Bertram, C., Dietrich, J.-P., Luderer, G., Pehl, M., Pietzcker, R.,
565 Piontek, F., Lotze-Campen, H., Biewald, A., Bonsch, M., Giannousakis, A., Kreidenweis, U., Müller, C., Rolinski,
566 S., Schultes, A., Schwanitz, J., Stevanovic, M., Calvin, K., Emmerling, J., Fujimori, S., and Edenhofer, O.: Fossil-
567 fueled development (SSP5): An energy and resource intensive scenario for the 21st century, Glob. Environ.
568 Change, 42, 297–315, <https://doi.org/10.1016/j.gloenvcha.2016.05.015>, 2017.
- 569 Li, W., Ciais, P., Han, M., Zhao, Q., Chang, J., Goll, D. S., Zhu, L., and Wang, J.: Bioenergy Crops for Low
570 Warming Targets Require Half of the Present Agricultural Fertilizer Use, Environ. Sci. Technol., 55, 10654–
571 10661, <https://doi.org/10.1021/acs.est.1c02238>, 2021.
- 572 Liddicoat, S. K., Wiltshire, A. J., Jones, C. D., Arora, V. K., Brovkin, V., Cadule, P., Hajjima, T., Lawrence, D.
573 M., Pongratz, J., and Schwinger, J.: Compatible Fossil Fuel CO₂ Emissions in the CMIP6 Earth System Models’
574 Historical and Shared Socioeconomic Pathway Experiments of the Twenty-First Century, J. Climate, 34, 2853–
575 2875, <https://doi.org/10.1175/JCLI-D-19-0991.1>, 2021.
- 576 Meinshausen, M., Nicholls, Z. R. J., Lewis, J., Gidden, M. J., Vogel, E., Freund, M., Beyerle, U., Gessner, C.,
577 Nauels, A., Bauer, N., Canadell, J. G., Daniel, J. S., John, A., Krummel, P. B., Luderer, G., Meinshausen, N.,
578 Montzka, S. A., Rayner, P. J., Reimann, S., Smith, S. J., van den Berg, M., Velders, G. J. M., Vollmer, M. K., and
579 Wang, R. H. J.: The shared socio-economic pathway (SSP) greenhouse gas concentrations and their extensions to
580 2500, Geosci. Model Dev., 13, 3571–3605, <https://doi.org/10.5194/gmd-13-3571-2020>, 2020.
- 581 Melnikova, I., Boucher, O., Cadule, P., Ciais, P., Gasser, T., Quilcaille, Y., Shiogama, H., Tachiiri, K., Yokohata,
582 T., and Tanaka, K.: Carbon cycle response to temperature overshoot beyond 2 °C – an analysis of CMIP6 models,
583 Earth’s Future, 9, e2020EF001967, <https://doi.org/10.1029/2020EF001967>, 2021.
- 584 Mohr, A. and Raman, S.: Lessons from first generation biofuels and implications for the sustainability appraisal
585 of second generation biofuels, Energy Policy, 63, 114–122, <https://doi.org/10.1016/j.enpol.2013.08.033>, 2013.
- 586 O’Neill, B. C., Tebaldi, C., Van Vuuren, D. P., Eyring, V., Friedlingstein, P., Hurtt, G., Knutti, R., Kriegler, E.,
587 Lamarque, J. F., Lowe, J., Meehl, G. A., Moss, R., Riahi, K., and Sanderson, B. M.: The Scenario Model
588 Intercomparison Project (ScenarioMIP) for CMIP6, Geosci. Model Dev., 9, <https://doi.org/10.5194/gmd-9-3461-2016>, 2016.
- 590 Pongratz, J., Reick, C. H., Houghton, R. A., and House, J. I.: Terminology as a key uncertainty in net land use
591 and land cover change carbon flux estimates, Earth Syst. Dynam., 5, 177–195, <https://doi.org/10.5194/esd-5-177-2014>, 2014.



- 593 Popp, A., Calvin, K., Fujimori, S., Havlik, P., Humpenöder, F., Stehfest, E., Bodirsky, B. L., Dietrich, J. P.,
594 Doelmann, J. C., Gusti, M., Hasegawa, T., Kyle, P., Obersteiner, M., Tabeau, A., Takahashi, K., Valin, H.,
595 Waldhoff, S., Weindl, I., Wise, M., Kriegler, E., Lotze-Campen, H., Fricko, O., Riahi, K., and van Vuuren, D. P.:
596 Land-use futures in the shared socio-economic pathways, *Glob. Environ. Change*, 42, 331–345,
597 <https://doi.org/10.1016/j.gloenvcha.2016.10.002>, 2017.
- 598 Riahi, K., van Vuuren, D. P., Kriegler, E., Edmonds, J., O'Neill, B. C., Fujimori, S., Bauer, N., Calvin, K., Dellink,
599 R., Fricko, O., Lutz, W., Popp, A., Cuaresma, J. C., Samir, K. C., Leimbach, M., Jiang, L., Kram, T., Rao, S.,
600 Emmerling, J., Ebi, K., Hasegawa, T., Havlik, P., Humpenöder, F., Silva, L. A. D., Smith, S., Stehfest, E., Bosetti,
601 V., Eom, J., Gernaat, D., Masui, T., Rogelj, J., Strefler, J., Drouet, L., Krey, V., Luderer, G., Harmsen, M.,
602 Takahashi, K., Baumstark, L., Doelman, J. C., Kainuma, M., Klimont, Z., Marangoni, G., Lotze-Campen, H.,
603 Obersteiner, M., Tabeau, A., and Tavoni, M.: The Shared Socioeconomic Pathways and their energy, land use,
604 and greenhouse gas emissions implications: An overview, *Glob. Environ. Change*, 42, 153–168,
605 <https://doi.org/10.1016/j.gloenvcha.2016.05.009>, 2017.
- 606 Rogelj, J., Shindell, D., Jiang, K., Fifita, S., Forster, P., Ginzburg, V., Handa, C., Kheshgi, H., Kobayashi, S.,
607 Kriegler, E., Mundaca, L., Séférian, R., Vilarino, M. V., Calvin, K., de Oliveira de Portugal Pereira, J. C.,
608 Edelenbosch, O., Emmerling, J., Fuss, S., Gasser, T., Gillett, N., He, C., Hertwich, E., Höglund-Isaksson, L.,
609 Huppmann, D., Luderer, G., Markandya, A., Meinshausen, M., McCollum, D., Millar, R., Popp, A., Purohit, P.,
610 Riahi, K., Ribes, A., Saunders, H., Schädel, C., Smith, C., Smith, P., Trutnevyte, E., Xu, Y., Zhou, W., Zickfeld,
611 K., Mitigation Pathways Compatible with 1.5°C in the Context of Sustainable Development. - In: Masson-
612 Delmotte, V., Zhai, P., Pörtner, H. O., Roberts, D., Skea, J., Shukla, P. R., Pirani, A., Moufouma-Okia, W., Péan,
613 C., Pidcock, R., Connors, S., Matthews, J. B. R., Chen, Y., Zhou, X., Zhou, M. I., Lonnoy, E., Maycock, T.,
614 Tignor, M., Waterfield, T. (Eds.), *Global warming of 1.5 °C*, (IPCC Special Report), Geneva: Intergovernmental
615 Panel on Climate Change, 93-174, 2018.
- 616 Schueler, V., Weddige, U., Beringer, T., Gamba, L., and Lamers, P.: Global biomass potentials under
617 sustainability restrictions defined by the European Renewable Energy Directive 2009/28/EC, *GCB Bioenergy*, 5,
618 652–663, <https://doi.org/10.1111/gcbb.12036>, 2013.
- 619 Schwinger, J. and Tjiputra, J.: Ocean Carbon Cycle Feedbacks Under Negative Emissions, *Geophys. Res. Lett.*,
620 45, 5062–5070, <https://doi.org/10.1029/2018GL077790>, 2018.
- 621 Séférian, R., Rocher, M., Guivarch, C., and Colin, J.: Constraints on biomass energy deployment in mitigation
622 pathways: the case of water scarcity, *Environ. Res. Lett.*, 13, 054011, <https://doi.org/10.1088/1748-9326/aabcd7>,
623 2018.
- 624 Séférian, R., Nabat, P., Michou, M., Saint-Martin, D., Voldoire, A., Colin, J., Decharme, B., Delire, C., Berthet,
625 S., Chevallier, M., Sénési, S., Franchisteguy, L., Vial, J., Mallet, M., Joetzjer, E., Geoffroy, O., Guérémy, J.-F.,
626 Moine, M.-P., Msadek, R., Ribes, A., Rocher, M., Roehrig, R., Salas-y-Méla, D., Sanchez, E., Terray, L., Valcke,
627 S., Waldman, R., Aumont, O., Bopp, L., Deshayes, J., Éthé, C., and Madec, G.: Evaluation of CNRM Earth
628 System Model, CNRM-ESM2-1: Role of Earth System Processes in Present-Day and Future Climate, *J. Adv.
629 Model Earth Sy.*, 11, 4182–4227, <https://doi.org/10.1029/2019MS001791>, 2019.
- 630 Sellar, A. A., Jones, C. G., Mulcahy, J. P., Tang, Y., Yool, A., Wiltshire, A., O'Connor, F. M., Stringer, M., Hill,
631 R., Palmieri, J., Woodward, S., Mora, L. de, Kuhlbrodt, T., Rumbold, S. T., Kelley, D. I., Ellis, R., Johnson, C.
632 E., Walton, J., Abraham, N. L., Andrews, M. B., Andrews, T., Archibald, A. T., Berthou, S., Burke, E., Blockley,
633 E., Carslaw, K., Dalvi, M., Edwards, J., Folberth, G. A., Gedney, N., Griffiths, P. T., Harper, A. B., Hendry, M.
634 A., Hewitt, A. J., Johnson, B., Jones, A., Jones, C. D., Keeble, J., Liddicoat, S., Morgenstern, O., Parker, R. J.,
635 Predoi, V., Robertson, E., Siahaan, A., Smith, R. S., Swaminathan, R., Woodhouse, M. T., Zeng, G., and
636 Zerroukat, M.: UKESM1: Description and Evaluation of the U.K. Earth System Model, *J. Adv. Model Earth Sy.*,
637 11, 4513–4558, <https://doi.org/10.1029/2019MS001739>, 2019.
- 638 Shukla, P. R., Skea, J., Calvo Buendia, E., Masson-Delmotte, V., Pörtner, H. O., Roberts, D. C., Zhai, P., Slade,
639 R., Connors, S., and Van Diemen, R.: IPCC, 2019: Climate Change and Land: an IPCC special report on climate
640 change, desertification, land degradation, sustainable land management, food security, and greenhouse gas fluxes
641 in terrestrial ecosystems, 2019.



- 642 Smith, P., Davis, S. J., Creutzig, F., Fuss, S., Minx, J., Gabrielle, B., Kato, E., Jackson, R. B., Cowie, A., and
643 Kriegler, E.: Biophysical and economic limits to negative CO₂ emissions, *Nat. Clim. Change*, 6, 42–50,
644 <https://doi.org/10.1038/nclimate2870>, 2016.
- 645 Swart, N. C., Cole, J. N. S., Kharin, V. V., Lazare, M., Scinocca, J. F., Gillett, N. P., Anstey, J., Arora, V.,
646 Christian, J. R., Hanna, S., Jiao, Y., Lee, W. G., Majaess, F., Saenko, O. A., Seiler, C., Seinen, C., Shao, A.,
647 Sigmond, M., Solheim, L., von Salzen, K., Yang, D., and Winter, B.: The Canadian Earth System Model version
648 5 (CanESM5.0.3), *Geosci. Model Dev.*, 12, 4823–4873, <https://doi.org/10.5194/gmd-12-4823-2019>, 2019.
- 649 Tanaka, K., Boucher, O., Ciais, P., Johansson, D. J. A., and Morfeldt, J.: Cost-effective implementation of the
650 Paris Agreement using flexible greenhouse gas metrics, *Sci Adv*, 7, eabf9020,
651 <https://doi.org/10.1126/sciadv.abf9020>, 2021.
- 652 Whitaker, J., Field, J. L., Bernacchi, C. J., Cerri, C. E. P., Ceulemans, R., Davies, C. A., DeLucia, E. H., Donnison,
653 I. S., McCalmont, J. P., Paustian, K., Rowe, R. L., Smith, P., Thornley, P., and McNamara, N. P.: Consensus,
654 uncertainties and challenges for perennial bioenergy crops and land use, *GCB Bioenergy*, 10, 150–164,
655 <https://doi.org/10.1111/gcbb.12488>, 2018.
- 656 Wu, D., Piao, S., Zhu, D., Wang, X., Ciais, P., Bastos, A., Xu, X., and Xu, W.: Accelerated terrestrial ecosystem
657 carbon turnover and its drivers, *Globa. Change Biol.*, 26, 5052–5062, <https://doi.org/10.1111/gcb.15224>, 2020.
- 658



659 **Tables & figures**

660

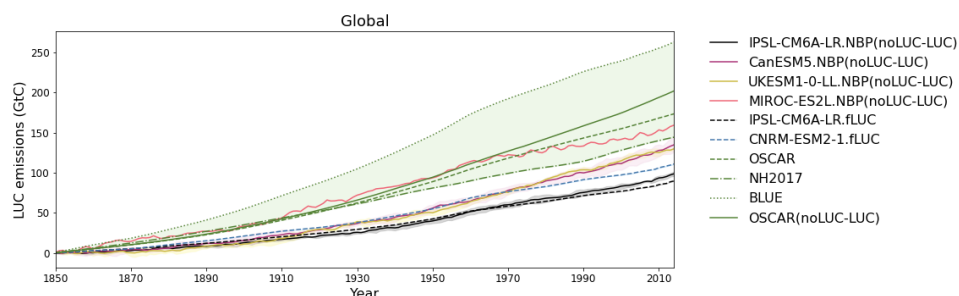
661 **Table 1. Major characteristics of the Earth system models.**

ESM*	Reference	Land carbon model	Resolution (land)	Inclusion of “fLuc”	Processes included to “fLuc”
IPSL-CM6A-LR	(Boucher et al., 2020)	ORCHIDEE, br.2.0	144 × 143	Yes	deforestation decomposition
CNRM-ESM2-1	(Séférian et al., 2019)	ISBA-CTRIP	256 × 128	Yes	deforestation decomposition
CanESM5	(Swart et al., 2019)	CLASS-CTEM	128 × 64	No	
UKESM1-0-LL	(Sellar et al., 2019)	JULES-ES-1.0	192 × 144	Yes (excluded)	deforestation wood harvest decomposition
MIROC-ES2L	(Hajima et al., 2020)	VISIT-e	128 × 64	No	

662 *DOIs of simulations by each ESM are provided in Table S1.

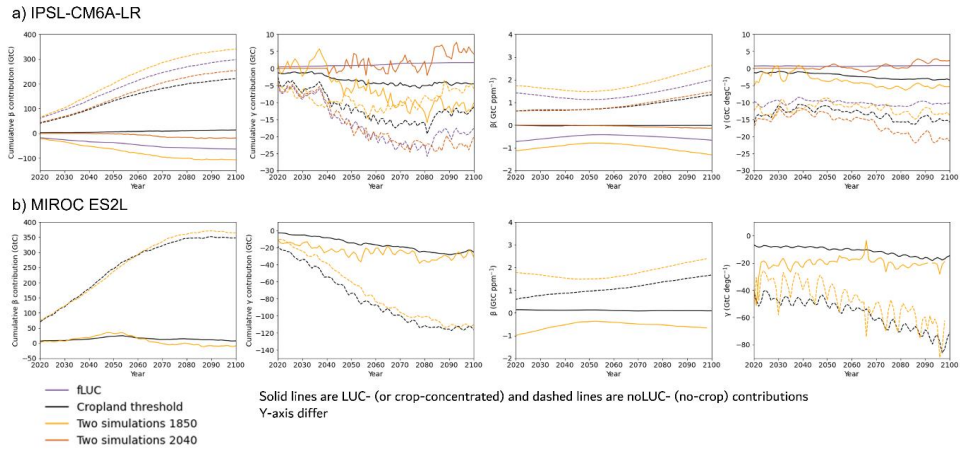
663

664



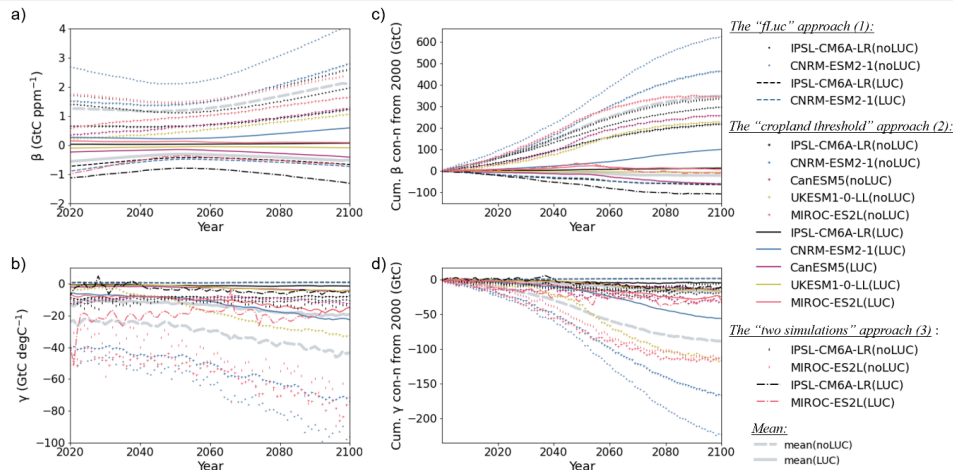
665

666 **Figure 1: Evaluation of cumulative global LUC emissions by ESMs against three bookkeeping models. LUC emissions**
 667 **are defined by two methods: 1) the difference in NBP between simulations with and without LUC (solid lines) and 2)**
 668 **the “fLuc” variable provided in CMIP6 (dashed lines). The estimates of bookkeeping approach using OSCAR are**
 669 **shown for cases with (noLUC-LUC) and without LASC). The range of bookkeeping models is in shaded green.**

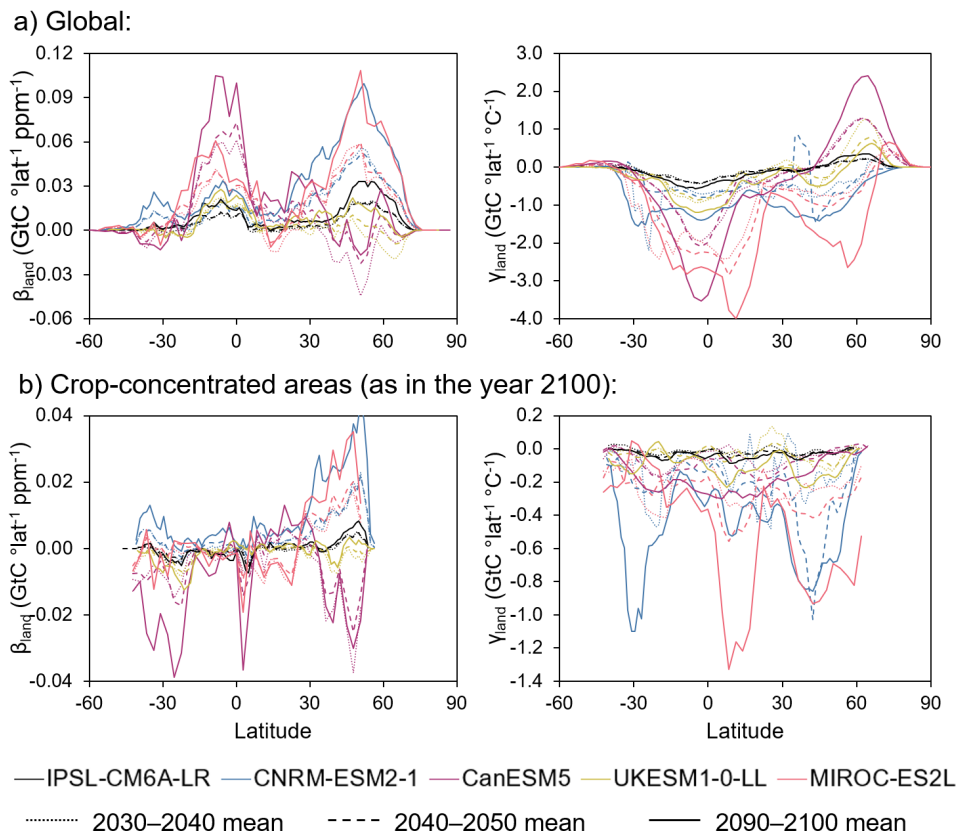


670
 671 **Figure 2: Differences in the impact of LUC on carbon cycle estimated by three approaches by (a) IPSL-CM6A-LR and**
 672 **(b) MIROC-ES2L. From left to right: cumulative β and γ contributions to land carbon uptake, and global land β and**
 673 **γ feedback parameters in LUC-concentrated (solid lines) and noLUC (dashed lines) ecosystems.**

674



675
 676 **Figure 3: Global (a) β and (b) γ feedback parameters, and cumulative (c) β and (d) γ feedback contributions to land**
 677 **carbon uptake in LUC or crop-concentrated and noLUC or no-crop ecosystems by three approaches.**



678

679 **Figure 4: Latitudinal distributions of the land β and γ feedback parameters (a) globally and (b) in crop-concentrated**
 680 **areas in the SSP5-3.4-OS pathway by five CMIP6 ESMs used in this study. Parameters in crop-concentrated areas are**
 681 **calculated as means of values in the range of cropland thresholds defined in Text A1.**

682